INT. J. REMOTE SENSING, 2001, VOL. 22, NO. 13, 2479–2487

Assessing the potential of VEGETATION sensor data for mapping snow and ice cover: a Normalized Difference Snow and Ice Index

XIANGMING XIAO

Complex Systems Research Center, Institute for the Study of Earth, Oceans and Space, University of New Hampshire, Durham, NH 03824, USA

ZHENXI SHEN

Northwest Plateau Institute of Biology, Chinese Academy of Sciences, Xining, Qinghai Province, 810001, China

and XIAOGUAN QIN

Institute of Geology, Chinese Academy of Sciences, Beijing, 100001, China

(*Received 15 November 1999; in final form 1 June 2000*)

Abstract. The VEGETATION (VGT) sensor in SPOT 4 has four spectral bands that are equivalent to Landsat Thematic Mapper (TM) bands (blue, red, near-infrared and mid-infrared spectral bands) and provides daily images of the global land surface at a 1-km spatial resolution. We propose a new index for identifying and mapping of snow/ice cover, namely the Normalized Difference Snow/Ice Index (NDSII), which uses reflectance values of red and mid-infrared spectral bands of Landsat TM and VGT. For Landsat TM data, NDSII is calculated as $NDSII_{TM} = (TM3 - TM5)/(TM3 + TM5)$; for VGT data, NDSII is calculated as $NDSII_{VGT} = (B2 - MIR)/(B2 + MIR)$. As a case study we used a Landsat TM image that covers the eastern part of the Qilian mountain range in the Qinghai–Xizang (Tibetan) plateau of China. $NDSII_{TM}$ gave similar estimates of the area and spatial distribution of snow/ice cover to the Normalized Difference Snow Index ($NDSI = (TM2 - TM5)/(TM2 + TM5)$) which has been proposed by Hall *et al.* The results indicated that the VGT sensor might have the potential for operational monitoring and mapping of snow/ice cover from regional to global scales, when using $NDSII_{VGT}$.

1. Introduction

In mid- to high-latitudes and alpine regions snow and ice cover plays a vital role in regional climate. Snow and ice cover also provides water resources for many parts of the world, where people rely on snowmelt for irrigation of croplands and drinking water. Area and spatial distribution of snow and ice cover in alpine regions varies significantly over time, due to seasonal and interannual variations in climate (Zhen and Li 1998). Therefore, there is a need for monitoring the area and spatial distribution of snow and ice cover from landscape to global scales.

A number of earlier remote sensing studies have used Landsat Thematic Mapper (TM) data and explored various TM spectral bands to identify and map snow and

International Journal of Remote Sensing
ISSN 0143-1161 print/ISSN 1366-5901 online © 2001 Taylor & Francis Ltd
http://www.tandf.co.uk/journals
DOI: 10.1080/01431160010002902

ice cover (Hall *et al.* 1995, 1998, Bresjö Bronge and Bronge 1999, Sidjak and Wheate 1999). Landsat TM data have fine spatial resolution (30 m), but a long revisit time (16 days), which significantly constrains their use for monitoring snow and ice cover over time for large spatial domains. During the last few decades, operational mapping and monitoring of snow and ice cover at continental to global scales have been largely dependent upon NOAA Advanced Very High Resolution Radiometer (AVHRR) data (Robinson *et al.* 1993, Xu *et al.* 1993).

Successful launches and operation of the VEGETATION (VGT) sensor on the SPOT 4 satellite in March 1998 and the MODIS sensor on the Terra platform in December 1999 represent the beginning of a new era for spaceborne observation of land surface and vegetation. The VGT sensor has four spectral bands that are equivalent to Landsat TM bands (TM1, TM3, TM4 and TM5; see table 1) and provides daily images of the global land surface at 1-km spatial resolution. Spectral characteristics and spatial/temporal resolutions of VGT data may offer a new opportunity to map and monitor snow and ice cover from landscape to global scales. In this paper we propose a new index for identifying and mapping snow and ice cover, namely The Normalized Difference Snow and Ice Index (NDSII), which can be calculated using red and mid-infrared spectral bands of VGT data. We used Landsat TM data that have equivalent spectral bands of VGT to examine NDSII and compared it to another snow cover index, the Normalized Difference Snow Index (NDSI) proposed by Hall *et al.* (1995, 1998). Our objective is to determine whether NDSII could provide similar estimates of snow and ice cover in comparison with NDSI (Hall *et al.* 1995, 1998). This Landsat TM-based analysis will provide a preliminary assessment and lay down a sound basis for us to use VGT data for further assessing the potential of VGT data in operational mapping of snow/ice cover from regional to global scales.

2. Remote sensing indices for identifying and mapping snow and ice cover

Snow and ice cover have very high spectral reflectance values in the visible bands (TM1, 2, 3), but low reflectance values in the mid-infrared band (TM5) (figure 1). Among the four types of snow and ice cover with different grain sizes, the differences in spectral reflectance are relatively small in visible bands but large in mid-infrared band (figure 1). Hall *et al.* (1995, 1998) proposed the NDSI for identifying and mapping snow and ice cover. For TM data, NDSI is calculated using the reflectance values (Hall *et al.* 1995, 1998):

$$\mathrm{NDSI} = (\mathrm{TM2} - \mathrm{TM5})/(\mathrm{TM2} + \mathrm{TM5}) \quad (1)$$

Table 1. A comparison of VEGETATION (VGT) in SPOT 4, Landsat TM/Enhanced Thematic Mapper (ETM)+ and AVHRR sensors.

VGT (μm)	TM/ETM+ (μm)	AVHRR-11 (μm)
B0 (0.43–0.47)	TM1 (0.45–0.52)—Blue	
	TM2 (0.52–0.60)—Green	
B2 (0.61–0.68)	TM3 (0.63–0.69)—Red	CH1 (0.58–0.68)
B3 (0.78–0.89)	TM4 (0.76–0.90)—Near-infrared	CH2 (0.725–1.10)
MIR (1.58–1.75)	TM5 (1.55–1.75)—Mid-infrared	
Spatial resolution: 1 km	Spatial resolution: 30 m	Spatial resolution: 1 km
Revisit time: daily	Revisit time: 16 days	Revisit time: daily

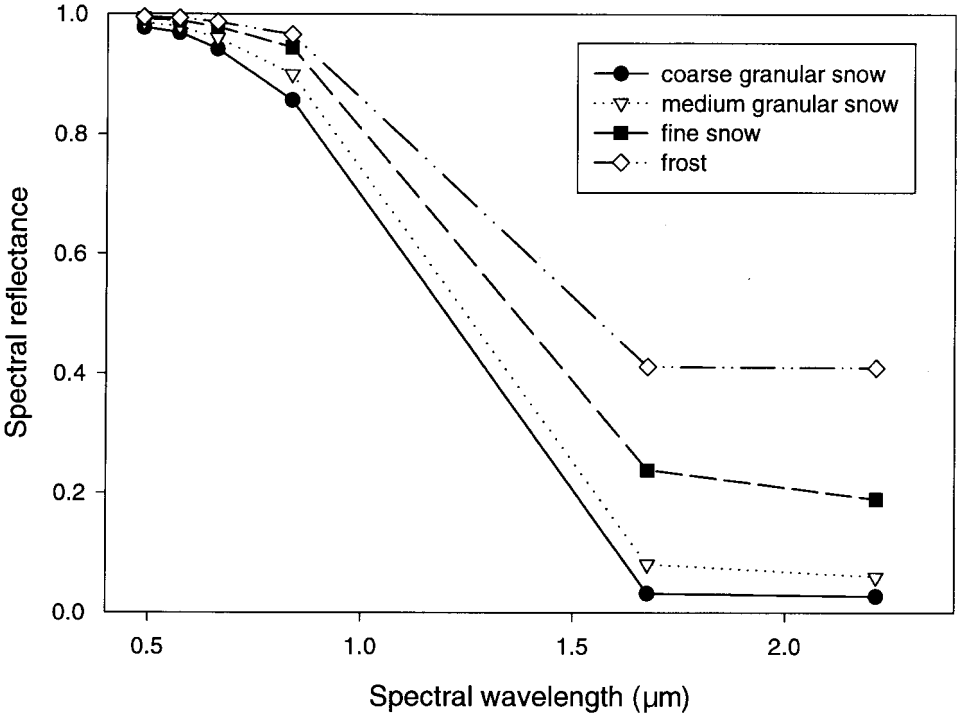

Figure 1. Spectral reflectance values of four types of snow and ice cover with different grain sizes, as measured in laboratory. The figure was generated after spectral re-sampling of the spectral library for snow and ice covers from the Johns Hopkins University, using Landsat 5 TM spectral bandwidths (see table 2). The ENVI software (version 3.2, Research System Inc.) provided the spectral library and spectral re-sampling algorithm. The reflectance values in the figure are for the mid-point of each spectral bands of Landsat TM and are the same as those in table 2.

The VGT sensor has no spectral band that is equivalent to TM2 band (the green wavelengths), and thus could not directly calculate NDSI for identifying and mapping snow and ice cover. However, the three visible bands (TM1, 2, 3) of Landsat TM are highly correlated with each other (figure 1), and other studies have suggested that TM3 is a useful spectral band for identifying snow and ice cover (Bresjö Bronge and Bronge 1999, Sidjak and Wheate 1999). For instance, in using Landsat TM data and ground radiometer measurements to classify ice and snow-type in the eastern Antarctic, Bresjö Bronge and Bronge (1999) found that the TM3/TM4 ratio is a simple tool for distinguishing between blue-ice and snow of various characters, and the TM3/TM5 ratio is a useful tool for quantifying snow grain-size variations. The VGT sensor has red and mid-infrared spectral bands that are equivalent to TM3 and TM5 (table 1). As indicated by the above Landsat TM studies (Bresjö Bronge and Bronge 1999, Sidjak and Wheate 1999), the red and mid-infrared bands in VGT may offer a new opportunity for large-scale mapping of snow and ice cover. Therefore, we propose a new index, the NDSII that uses reflectance values of red and mid-infrared bands of VGT data. For Landsat TM data, NDSII is calculated using the reflectance values:

$$\mathrm{NDSII}_{\mathrm{TM}} = (\mathrm{TM3} - \mathrm{TM5})/(\mathrm{TM3} + \mathrm{TM5}) \quad (2)$$

And for VGT data (table 1), NDSII is calculated using the reflectance values:

$$\mathrm{NDSII}_{\mathrm{VGT}} = (\mathrm{B2} - \mathrm{MIR})/(\mathrm{B2} + \mathrm{MIR}) \quad (3)$$

3. Description of Landsat TM data and the study area in Qinghai province, China

As a case study, we obtained a Landsat 5 TM image (Path 132/Row 34) acquired on 16 August 1996. As the standard product of Beijing Satellite Remote Sensing Ground Station in China, the TM image was geo-referenced and re-sampled to 25 m spatial resolution. We first converted the digital numbers (DN) of the seven-band TM image into extra-atmospheric reflectance values (reflectance above the atmosphere), using the published Landsat TM post-launch gains and offsets (see the Landsat TM calibration procedure in ENVI software version 3.2). The resultant reflectance image was then used for calculating NDSI and $\mathrm{NDSII}_{\mathrm{TM}}$ indices. A subset (1700 lines and 1800 pixels at 25 m resolution) of the TM image was used in this study (figure 2).

Our study area (101°25′E to 101°50′E and 37°30′N to 37°50′N) is located in Qinghai province of China (figure 3), to the north-west of the provincial capital, Xining city. The large mountain that stretches from south-east to north-west (figure 2) is the eastern part of the Qilian mountain range in the Qinghai–Xizang (Tibetan) plateau of China. The highest peak in the study area (5076 m high) has permanent snow cover. The perennial snow line is at an altitude of about 4200 m. The climate in the study area is alpine continental (Yang 1982). According to weather records from the local weather station (37°37′N, 101°19′E, 3250 m altitude) at the Alpine Meadow Ecosystem Research Station of the Chinese Academy of Sciences (Yang 1982), the annual mean temperature is about −2°C. Mean monthly temperature in January is −18°C and in July it is 10°C. Annual mean precipitation is about 530 mm, with 90% falling as rain in the warm season from April to November.

Natural vegetation in the study area is dominated by alpine shrub and alpine meadow (Zhou and Sun 1990, Su 1993). Dominant alpine shrub species are *Dasiphora fruticosa* and *Salix oritrepha*, which are widely distributed over the Qinghai–Xizang (Tibetan) Plateau (Zhou *et al.* 1987). Dominant species in alpine meadows are *Kobresia humilis*, *K. pygmaea*, *K. tibitica* and *K. capilifolia* (Zhou and Li 1982). Alpine vegetation, mostly distributed along an elevation gradient of 3000–3800 m, is primarily used as pasture for livestock grazing (Wu 1990). In the lower part of the image (figure 2) there is a large area of cropland at an elevation of about 2800 m.

4. Estimates of area and spatial distribution of snow and ice cover

Laboratory-based reflectance measurements for four types of snow/ice cover with different grain sizes shows large reflectance values in the visible spectral bands (TM1, TM2 and TM3), but very small reflectance values in the mid-infrared (TM5) band due to snow absorption (figure 1, table 2). This difference in reflectance values between the visible bands and the mid-infrared band results in large NDSI and $\mathrm{NDSII}_{\mathrm{TM}}$ values for snow/ice cover (table 2). There is little increase in reflectance values of TM2 and TM3 bands, but a relatively large increase in reflectance values of TM5 band from coarse granular snow to frost (figure 1). Thus, $\mathrm{NDSII}_{\mathrm{TM}}$ values range from 0.41 for frost to 0.94 for coarse granular snow (table 2). Generally, there is little difference between NDSI and $\mathrm{NDSII}_{\mathrm{TM}}$ values for these four types of snow/ice cover (table 2).

Figure 4 shows the spatial distributions of NDSI and $\mathrm{NDSII}_{\mathrm{TM}}$ in the study area.

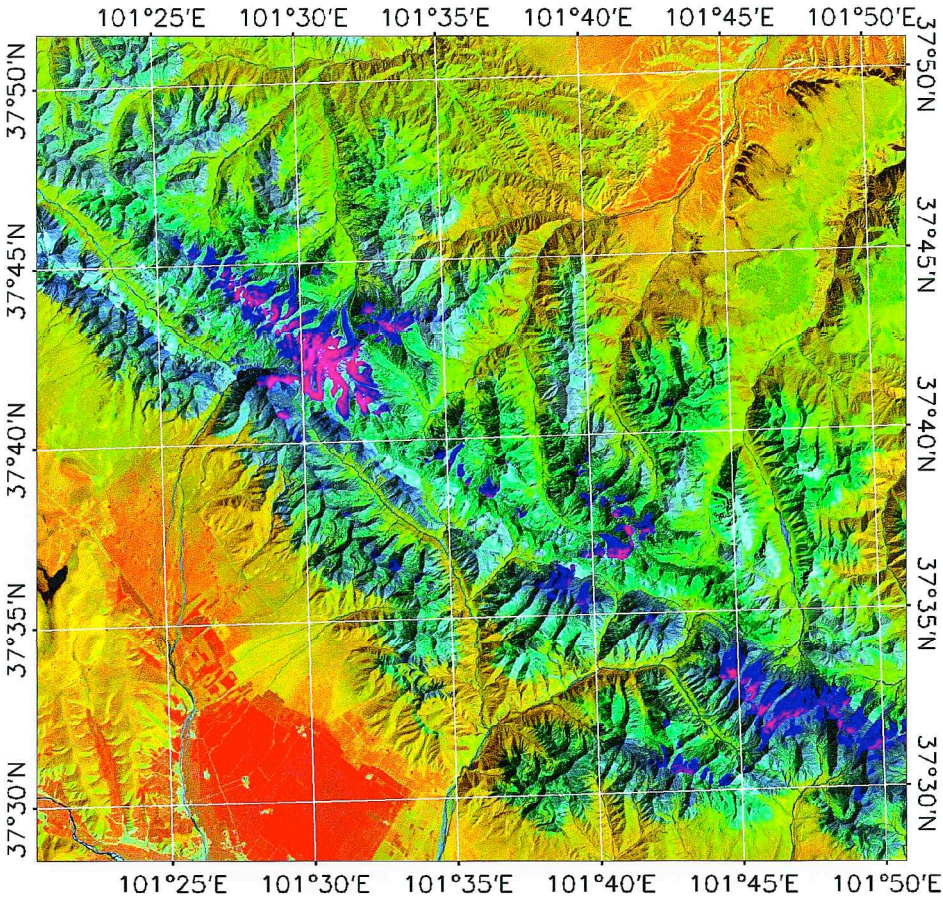

Figure 2. Land cover types in the study area of Qinghai province. The image is a false colour composite of a Landsat TM image acquired on 16 August 1996, TM4 (red), TM5 (green) and TM3 (blue). Snow and ice cover occurs mostly over the Qilian mountain range (pink colour along the north-west–south-east diagonal of the image). The area represented is 42.5 km by 45 km.

The very bright white areas in the Qilian mountain range have large values of NDSI and $NDSII_{TM}$ (mostly 0.7) and are likely to be snow/ice cover (figure 2). The spatial distribution of NDSI is very similar to the spatial distribution of $NDSII_{TM}$ (figure 4). Figure 5 illustrates a pixel-to-pixel comparison between NDSI and $NDSII_{TM}$ values, and it shows that NDSI is highly correlated with $NDSII_{TM}$, especially at higher NDSI and $NDSII_{TM}$ values (i.e. snow/ice cover).

Hall *et al.* (1998) suggested that a NDSI threshold of 0.40 be used to map snow cover. In this study, we adopted the same threshold for both NDSI and $NDSII_{TM}$. Using the NDSI threshold of 0.40, it is estimated that there is a snow/ice area of 85 387 pixels (about 53.37 km^2) in the study area (figure 4). Similarly, using the $NDSII_{TM}$ threshold of 0.40, it is estimated that there is a snow/ice area of 85 491 pixels (about 53.43 km^2) in the study area (figure 4), only 104 pixels (or 0.1%) more than that by NDSI. Thus, the difference in area estimates of snow/ice cover between NDSI and $NDSII_{TM}$ is negligible.

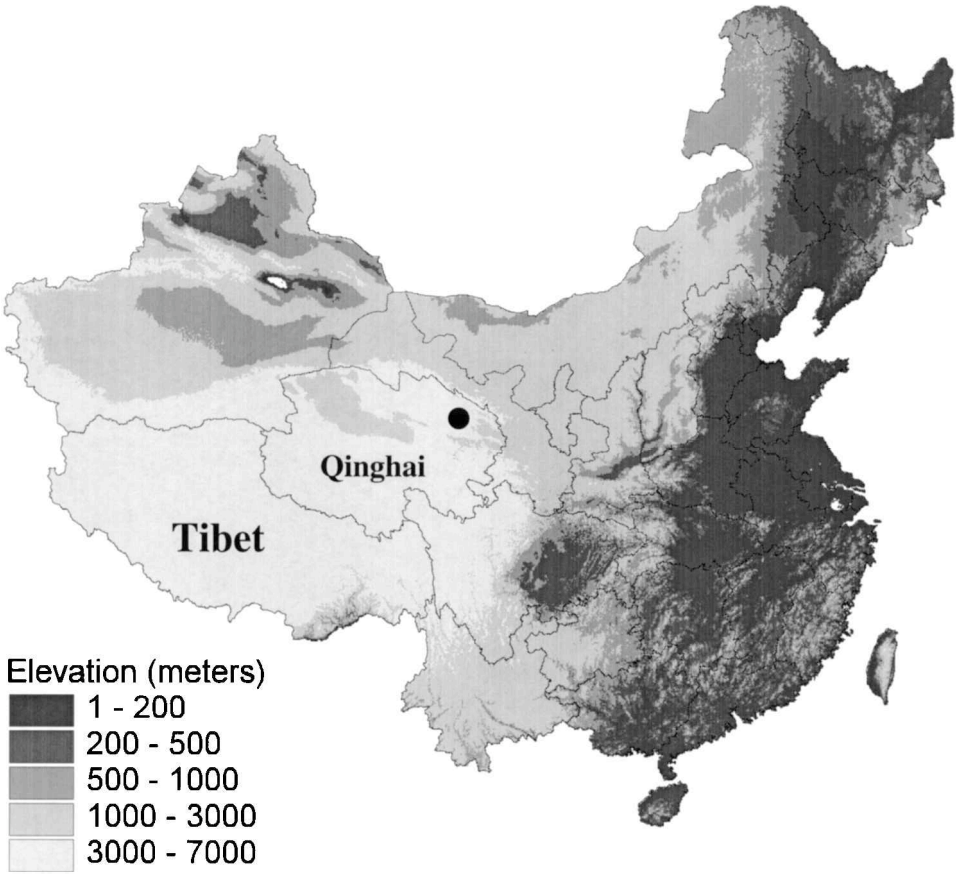

Figure 3. Approximate location of the study area within Qinghai province of China. The filled circle within Qinghai province represents the location of the study area.

Table 2. A comparison of NDSI and NDSII values among four types of snow/ice cover with different grain sizes. Note that spectral reflectance values of snow and ice cover are generated from the Johns Hopkins University's spectral library for snow types, using Landsat 5 TM spectral bandwidths. The ENVI software (version 3.2, Research System Inc.) provided the spectral library and the spectral re-sampling algorithm. The reflectance values in the table are for the mid-point of each spectral band and are the same as those in figure 1. NDSI = (TM2 − TM5)/(TM2 + TM5) and $NDSII_{TM}$ = (TM3 − TM5)/(TM3 + TM5).

	Spectral reflectance values of snow and ice cover			
Optical sensor Landsat TM (μm)	Coarse granular snow	Medium granular snow	Fine granular snow	Frost
TM1 (0.45–0.52)				
TM2 (0.52–0.60)	0.9687	0.9789	0.9887	0.9929
TM3 (0.63–0.69)	0.9416	0.9599	0.9781	0.9865
TM4 (0.76–0.90)				
TM5 (1.55–1.75)	0.0316	0.0805	0.2384	0.4111
NDSI (Hall *et al.* 1998, 1995)	0.937	0.848	0.611	0.414
$NDSII_{TM}$ (Xiao *et al.*, this study)	0.935	0.845	0.608	0.412

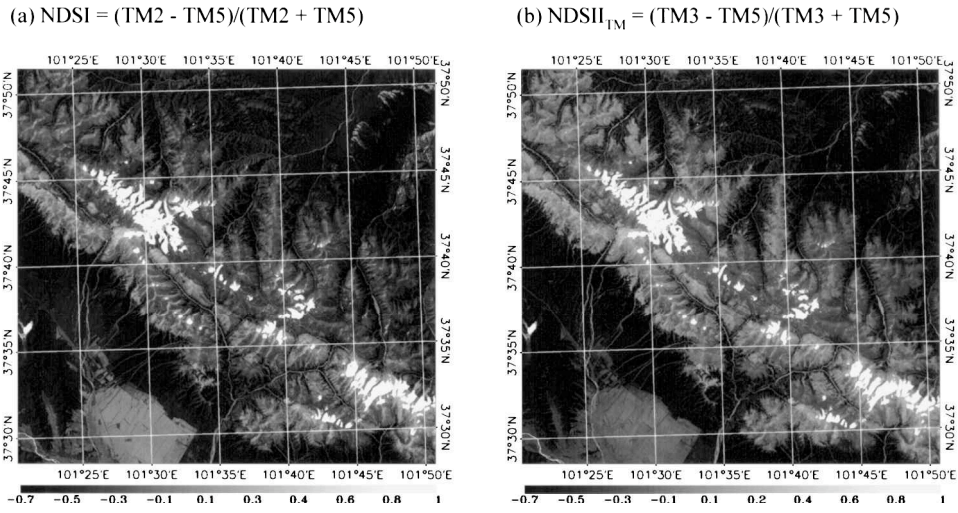

Figure 4. Spatial distributions of (*a*) the NDSI and (*b*) the NDSII$_{TM}$, as calculated from a Landsat TM image acquired on 16 August 1996.

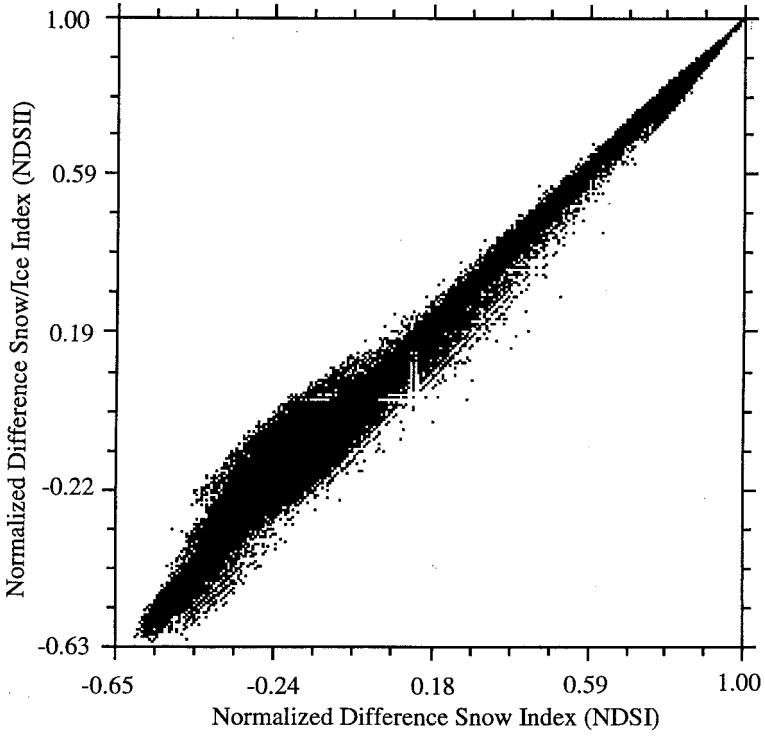

Figure 5. Comparison between the NDSI and the NDSII$_{TM}$, as calculated from a Landsat TM image acquired on 16 August 1996, for 160 000 pixels from a 400 by 400 pixel subset image centred at 101°30′E and 37°42′N. This subregion contains the snow/ice area shown in north-western part of figure 4.

5. Conclusion

This Landsat TM-based case study for alpine snow/ice cover in the Qinghai–Xizang (Tibetan) plateau shows that $NDSII_{TM}$ provides similar estimates of area and spatial distribution of snow/ice cover as NDSI (Hall *et al.* 1995, 1998). Note that this TM image was acquired on 16 August 1996, when snow/ice cover was likely to have been near its annual minimum. Multitemporal remote sensing data will be required for quantifying spatial–temporal dynamics of snow/ice cover.

The implication of this study is that NDSII might be a useful index for operational mapping and monitoring of snow/ice cover, using daily or 10-day synthetic VGT data that are already available. We are currently analysing multitemporal 10-day synthetic VGT data acquired in 1999 and exploring the potential of NDSII for mapping of snow/ice cover in the Qinghai–Xizang (Tibetan) plateau, China. The results are reported in another paper (Xiao *et al.* 2000).

Acknowledgements

This study was supported by the NASA EOS interdisciplinary project and the NASA/NSF/DOE/USDA/NOAA Joint Program on Terrestrial Ecology and Global Change (TECO). Z. Shen and X. Qin are visiting scholars at the Complex Systems Research Center, Institute for the Study of Earth, Oceans and Space, University of New Hampshire, under the support of the Chinese Academy of Sciences. We thank Stephen Frolking and Stephen Boles for their help on the manuscript. We also thank the three anonymous reviewers for their insightful comments and suggestions on the earlier version of the manuscript.

References

Bresjö Bronge, L. B., and Bronge, C., 1999, Ice and snow-type classification in the Vestfold Hills, East Antarctica, using Landsat TM data and ground radiometer measurements. *International Journal of Remote Sensing*, **2**, 225–240.

Hall, D. K., Riggs, G. A., and Salomonson, V. V., 1995, Development of methods for mapping global snow cover using moderate resolution imaging spectroradiometer data. *Remote Sensing of Environment*, **54**, 27–140.

Hall, D. K., Foster, J. L., Verbyla, D. L., and Klein, A. G., 1998, Assessment of snow-cover mapping accuracy in a variety of vegetation-cover densities in central Alaska. *Remote Sensing of Environment*, **66**, 129–137.

Robinson, D. A., Dewey, K. F., and Heim, R. R., 1993, Global snow cover monitoring: an update. *Bulletin of American Meteorological Society*, **74**, 1689–1696.

Sidjak, R. W., and Wheate, R. D., 1999, Glacier mapping of the Illecillewaet icefield, British Columbia, Canada, using Landsat TM and digital elevation data. *International Journal of Remote Sensing*, **2**, 273–284.

Su, D. (ed.), 1993, *The Atlas of Grassland Resources of China* (1:1 000 000). (Beijing, China: Press of Map) (in Chinese).

Wu, C. (ed.), 1990, *Land Use Map of China* (1:1 000 000) (Beijing, China: Science Press) (in Chinese).

Xiao, X., Moore, B., Qin, X., Shen, Z., and Boles, S., 2000, Large-scale observation of alpine snow and ice cover in Asia: using image data from VEGETATION sensor in SPOT 4. Submitted to *International Journal of Remote Sensing*.

Xu, H., Bailey, J. O., Barrett, E. C., and Kelly, R. E. J., 1993, Monitoring snow area and depth with integration of remote sensing and GIS. *International Journal of Remote Sensing*, **14**, 3259–3268.

Yang, F., 1982, A general view of the natural geography in the region of the research station of Alpine Meadow Ecosystem. In *Alpine Meadow Ecosystem*, vol. 1, edited by W. Xia (China: Gansu People's Publishing House), pp. 1–6 (in Chinese).

ZHOU, L., and SUN, S. (eds), 1990, *Vegetation Map of Qinghai Province, China* (1:1 000 000) (Beijing: Press of Science and Technology) (in Chinese).

ZHOU, X., WANG, Z., and DU, Q., 1987, *Vegetation in Qinghai Province, China*. (Xining, Qinghai province, China: People's Press), pp. 199 (in Chinese).

ZHOU, X., and LI, J., 1982, The major vegetation types and their geographical distribution at the Haibei Research Station of Alpine Meadow Ecosystem, Menyuan county, Qinghai province. In *Alpine Meadow Ecosystem*, vol. 1, edited by W. Xia (China: Gansu People's Publishing House), pp. 9–18 (in Chinese).

ZHEN, Q., and LI, Z., 1998, Remote sensing monitoring of glaciers, snow and lake ice in Qinghai–Xizang (Tibetan) Plateau. In *Contemporary Climatic Variations over Qinghai-Xizang (Tibetan) Plateau and their Influences on Environments*, edited by M. Tang, G. Cheng and Z. Lin (Guangzhou, China: Guangdong Science and Technology Press), pp. 279–308 (in Chinese).